THE ROLE OF SILICATE MINERAL ALTERATION IN THE SUPERGENE ENRICHMENT PROCESS

by

Dianne Catherine Marozas

A Thesis Submitted to the Faculty of the

DEPARTMENT OF GEOSCIENCES

In Partial Fulfillment of the Requirements
For the Degree of

MASTER OF SCIENCE

In the Graduate College

THE UNIVERSITY OF ARIZONA

1 9 8 2

STATEMENT BY AUTHOR

This thesis has been submitted in partial fulfillment of requirements for an advanced degree at The University of Arizona and is deposited in the University Library to be made available to borrowers under rules of the Library.

Brief quotations from this thesis are allowable without special permission, provided that accurate acknowledgement of source is made. Requests for permission for extended quotations from or reproduction of this manuscript in whole or in part may be granted by the head of the major department or the Dean of the Graduate College when in his judgement the proposed use of the material is in the interests of scholarship. In all other instances, however, permission must be obtained from the author.

SIGNED: Dianne C. Marajas

APPROVAL BY THESIS DIRECTOR

This thesis has been approved on the date shown below:

Spencer R Titley
S. R. Titley
Professor of Geosciences

13th Dec. 1982
Date

ACKNOWLEDGEMENTS

I am most grateful to my major advisor, Dr. Spencer R. Titley for his unfailing support and guidance throughout this project. I would also like to thank Dr. Dennis Norton and Dr. J. F. Schreiber, Jr. for reviewing the manuscript and providing valuable suggestions for its improvement.

I also wish to express my appreciation to ASARCO Corporation for providing core samples and generous financial support without which this study would not be possible.

I would like to dedicate this work to Dr. Robert M. Garrels, a most 'benevolent oligarch,' who serves both as an inspiration and a guide in my career as a geologist.

TABLE OF CONTENTS

LIST OF TABLES

LIST OF ILLUSTRATIONS

Page

ABSTRACT

A detailed mineralogic and quantitative chemical study of rocks and mine waters from Silver Bell Mine, Silver Bell, Arizona, provides a basis for describing silicate reactions in the weathering of a copper porphyry deposit and for determining the influences these reactions have on copper enrichment.

Electron microprobe results indicate that concentrations of all cations except aluminum, silicon, and potassium decrease within sericite mineral structures as the effects of weathering become more intense. This data implies that structural site leaching is a significant means of mineral alteration in the supergene zone.

Silicate weathering reactions consume hydrogen ion and release gangue cations. Both of these effects tend to stabilize copper minerals within the oxidized zone and therefore inhibit copper migration and subsequent enrichment. The efficiency of copper enrichment then is a function not only of the total sulfide available but also depends on the reactivity of silicate minerals in the host rock.

CHAPTER 1

INTRODUCTION AND PREVIOUS WORK

During the supergene enrichment of metal sulfide bearing rock, meteoric water leaches, transports, and redeposits cations as it percolates downward as part of the natural weathering cycle. By this process copper is concentrated into ore grade levels from low grade hypogene mineralization in many porphyry deposits. This study examines the systematics of the secondary alteration of silicate minerals within the supergene process and the chemical influences that silicate alteration have on metal enrichment.

In the enrichment process minerals such as pyrite and chalcopyrite are oxidized in the presence of free oxygen available in meteoric water, a reaction which releases H^+ and free metal to solution (eqs. 1 & 2). The copper metal ion is transported by solution to reducing environments and

$$1)\ \overset{\text{solid}}{CuFeS_2} + 4\tfrac{1}{4}O_2 + 1\tfrac{1}{2}H_2O = \overset{\text{solid}}{FeOOH} + Cu^{2+} + 2SO_4 + H^+$$

$$2)\ \overset{\text{solid}}{FeS_2} + 3\tfrac{1}{4}O_2 + \tfrac{1}{2}H_2 = Fe^{3+} + 2SO_4^{2-} + H^+$$

precipitates primarily as chalcocite by reaction with hypogene sulfides to form an enriched zone of copper mineralization.

Through extensive field analysis of sulfide systems Emmons (1917) describes three distinct zones common in enriched sulfide deposits. The oxidized zone is where, in the presence of oxygenated solution, sulfide and gangue minerals break down to soluble salts and free metal ions to form minerals stable in environments with high oxidations potentials. Dissolution generally exceeds precipitation and the solution removes material from this zone. Typically at present or remnant ground water levels there is a sharp transition between the oxidized zone and a zone where reduced sulfides are stable called the enriched zone. The thickness of this zone although richest in ore at shallow depths varies with individual deposits depending on local climatic conditions, permeability, and on sulfide content and mineralogy of the host rock. Below the enriched zone is the protore zone where primary metal sulfides exist unchanged or unconcentrated by weathering processes.

Because the solubility of copper minerals is a function of pH and Eh, stability fields can be plotted on diagrams, (Garrels 1954), that accurately represent mineral associations observed in the field. Mineral relationships in Figure 1 emphasize the important role that oxidation potential plays in the deposition of copper in secondarily

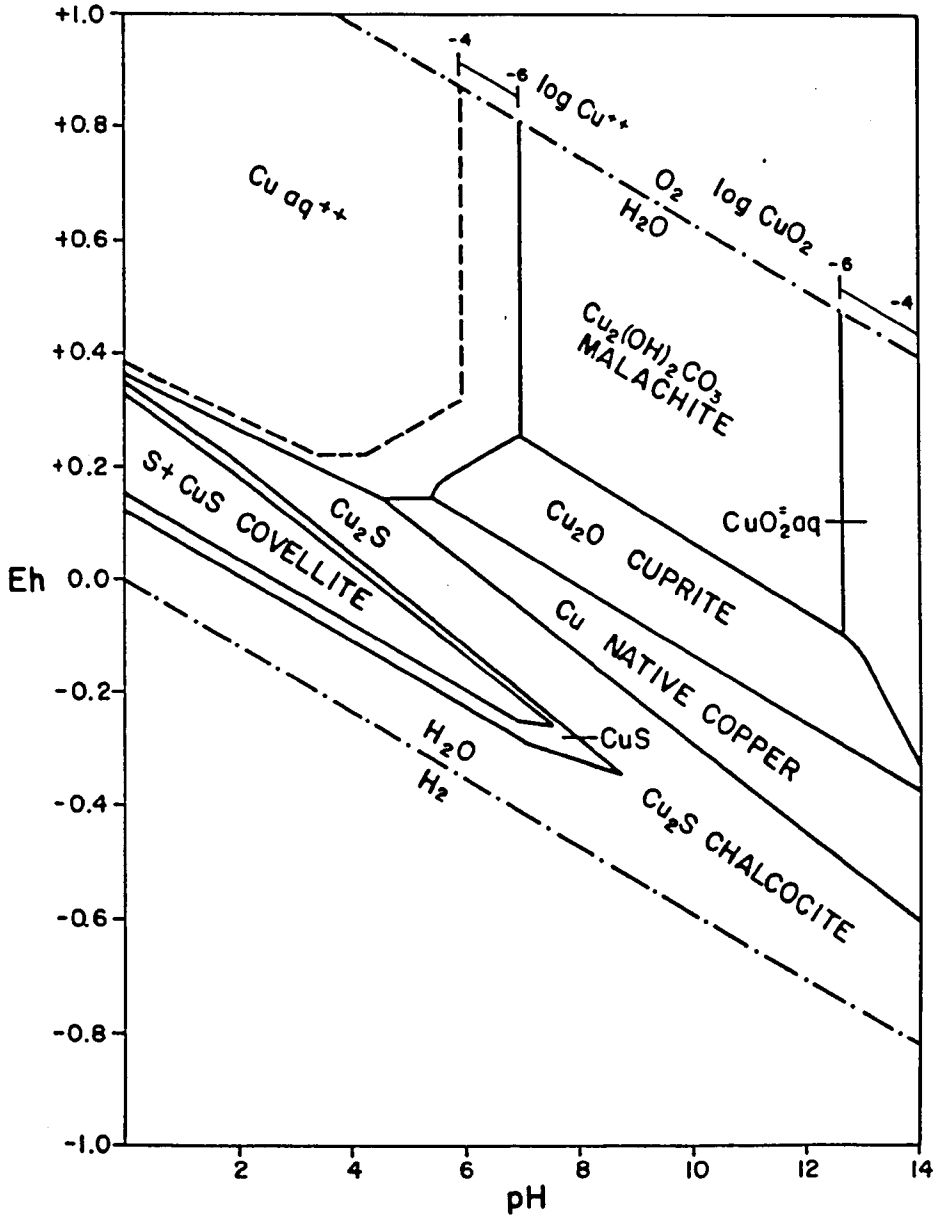

Figure 1. Stability fields of copper minerals in the system $Cu-H_2O-O_2-S-CO_2$ at 25°C and 1 atmosphere, $P_{CO_2} = 10^{-35}$, and total dissolved sulfur $= 10^{-1}$, showing the effects of an increase in copper concentration on mineral stabilities from Garrels and Christ (1968) p. 240.

enriched systems, where changes in Eh are accompanied by changes in sulfide mineral stabilities. Metal sulfides are stable under reducing conditions but they liberate metal cations and sulfate ligand under oxidizing conditions. Acidity is also a controlling function of mineral stability and metal leaching. At higher pH (Figure 1) copper minerals will precipitate even in the presence of high oxidation potentials, at low pH values, however, copper solubility increases and ions can move from the oxidized zone. Therefore, the amount of leaching and subsequent enrichment is directly proportional to the amount of sulfide minerals available that are able to produce free sulfuric acid and is inversely related to the reactivity of gangue minerals in the host rock environment (Posnak and Merwin 1922, Blanchard 1968).

Host rock with high total volume percent sulfide values will yield high concentrations of sulfuric acid upon oxidation which decreases pH and increases ligand concentration of solutions within the oxidized zone. An increase in copper sulfide to iron sulfide ratio or an increase in the weight percent copper in hypogene copper sulfide minerals tends to lower the amount of sulfuric acid produced during oxidation. Anderson (1982) empirically determined correlations between the mass ratio of goethite in limonite in the leached capping to total volume percent sulfide and to the copper-sulfide to iron-sulfide ratios in unweathered rock.

Anderson's data indicates that sulfide deposits with low (1½ percent) total sulfide or high Cu/Cu-sulfide ratios are not capable of leaching significant amounts of copper or iron from the oxidized zone. However, sulfide deposits with high sulfide and low Cu/Cu-sulfide ratios are capable of leaching most of the metal cations from the oxidized zone.

Bladh (1982) simulated weathering reactions between sulfide-silicate mineral assemblages and meteoric solutions by using numerical approximations of the differential equations that describe the system. Bladh found that at constant temperature, pressure, pH, sulfate, and potassium concentration, the relative order of jarosite and alunite precipitation depends on the relative amounts of iron and aluminum available in solution. His experiments show that the reaction product (jarosite and alunite) depends on the mole ratio of Fe/Al in solution, where values less than .5 generate alunite, values greater than 1.0 generate jarosite, and both precipitate between .5 and 1.0. Iron is available to solution from the oxidation of iron sulfide minerals and aluminum is a product of the dissolution of silicate gangue. Bladh suggests that the amount of alunite produced is directly proportional to the extent of aluminosilicate dissolution and as such is an indicator of the thoroughness of silicate alteration.

Bladh also finds that reactions with low silicate to sulfide reaction rate ratios produced the same mineral

assemblage of mixed jarosite-goethite with only minor alunite that is commonly observed in leached cappings that overlie secondarily enriched copper deposits. Based on these simulations of chemical weathering and the fact that continued reaction of silicate minerals after total oxidation of sulfide forms alunite and goethite but dissolves jarosite, Bladh suggests that the precipitation of goethite and jarosite in the capping is separated spatially or temporally from acid consumptive silicate alteration reactions either because of slow kinetics of the silicate reactions or because of flow rates that hinder jarosite and goethite dissolution. Bladh, therefore, concludes that an enrichment process in which only minimal silicate alteration occurs before total oxidation of all sulfides is most representative of the supergene system.

However, the equilibration of silicate clay minerals with solutions especially under acidic conditions is found to be geologically fast under laboratory conditions. Clemency and Lin (1981) in an experiment on the reaction kinetics of phlogopite under low temperature, low pressure, and open system conditions with a pH range from 3-5, found that 36 percent of the initial solid was dissolved after 1000+ hours with a rate of 12 percent/hour for the first 200 hours. Obviously the reactivity of aluminosilicate minerals in the host rock has the potential to exert an important local control on the effectiveness of supergene enrichment.

Blanchard (1968) recognized that host rocks with mineral components that are unreactive in acid such as quartz, kaolinite, or sericite have practically no effects on supergene solutions. Whereas rocks composed of feldspars or ferromagnesion minerals have a much higher capacity for neutralization of acidic solutions.

Significant secondary concentration of copper sulfide in potassium silicate rocks occurs only in zones of quartz-sericite-pyrite or phyllic hypogene alteration. In phyllic alteration zones not only have high concentrations of pyrite provided excess sulfuric acid but the silicates are also less reactive in an acid environment because of the effects of hypogene hydrogen metasomatism. There are few reports of important supergene enrichment of copper above zones of potassic or propylitic alteration in potassium silicate rocks. Also, secondary sulfide enrichment does not develop extensively in calc-silicate, skarn altered, or mafic host rock systems (Titley 1982, Emmons 1917). Evidently supergene metal enrichment favors environments where there is an abundance of excess sulfuric acid and where the host rock silicate minerals are most stable in the presence of acidic solutions.

The chemical effects that silicate alteration have on metal enrichment beyond that of an acid consumer have not been well descibed with the exception of the studies of E.C. Sullivan. Sullivan (1905) found experimentally that

acid copper sulfate solutions in the presence of finely ground silicates would react to precipitate copper, would leach cations from the silicates into solution, and would not alter the acidity of the solution. From these results Sullivan suggested a possible mechanism for the precipitation of supergene copper in the enriched zone. His hypothesis of supergene enrichment was generally ignored because the method of oxidation and reduction more adequately explained the deposition of enriched copper sulfides. However, the conditions of Sullivan's experiment commonly exist in nature and the reactions that he described remain important in the alteration of silicates in the presence of acid copper sulfate solutions.

This study will focus on the low-temperature alteration of silicates in porphyry deposits. Knowledge of what role the silicates play in secondary enrichment of copper can be used to explain why certain sulfide rich deposits are enriched and others are not and can be used to improve the process of solution mining of copper by in situ leaching.

CHAPTER 2

RESEARCH METHODS AND RESULTS

I. Area of Study.

Rocks used for this study are from drill hole #358 just outside of the El Tiro pit, Silver Bell Mine, Silver Bell, Arizona. The Silver Bell Mining District is located 35 miles northwest of Tucson (Figure 2) and exhibits a classic example of supergene enrichment in porphyry sulfide deposits. The 20 samples collected are representative of typical conditions present in the oxidized, enriched, and protore zones of the 700+ feet of drill core recovered.

II. Lithology and Petrography.

The drill hole is located in Mesozoic alaskite porphyry rock that underlies the western half of the El Tiro pit. Unaltered, the alaskite is a buff. medium to coarse-grained, equigranular intrusion containing 25 percent quartz, 54 percent perthitic orthoclase, 18 percent oligoclase, 2 percent biotite, and minor accessories (Graybeal 1982). Hydrothermal alteration of the alaskite is dominantly of the phyllic type consisting of quartz, sericite, and pyrite. Within areas of strongest phyllic alteration

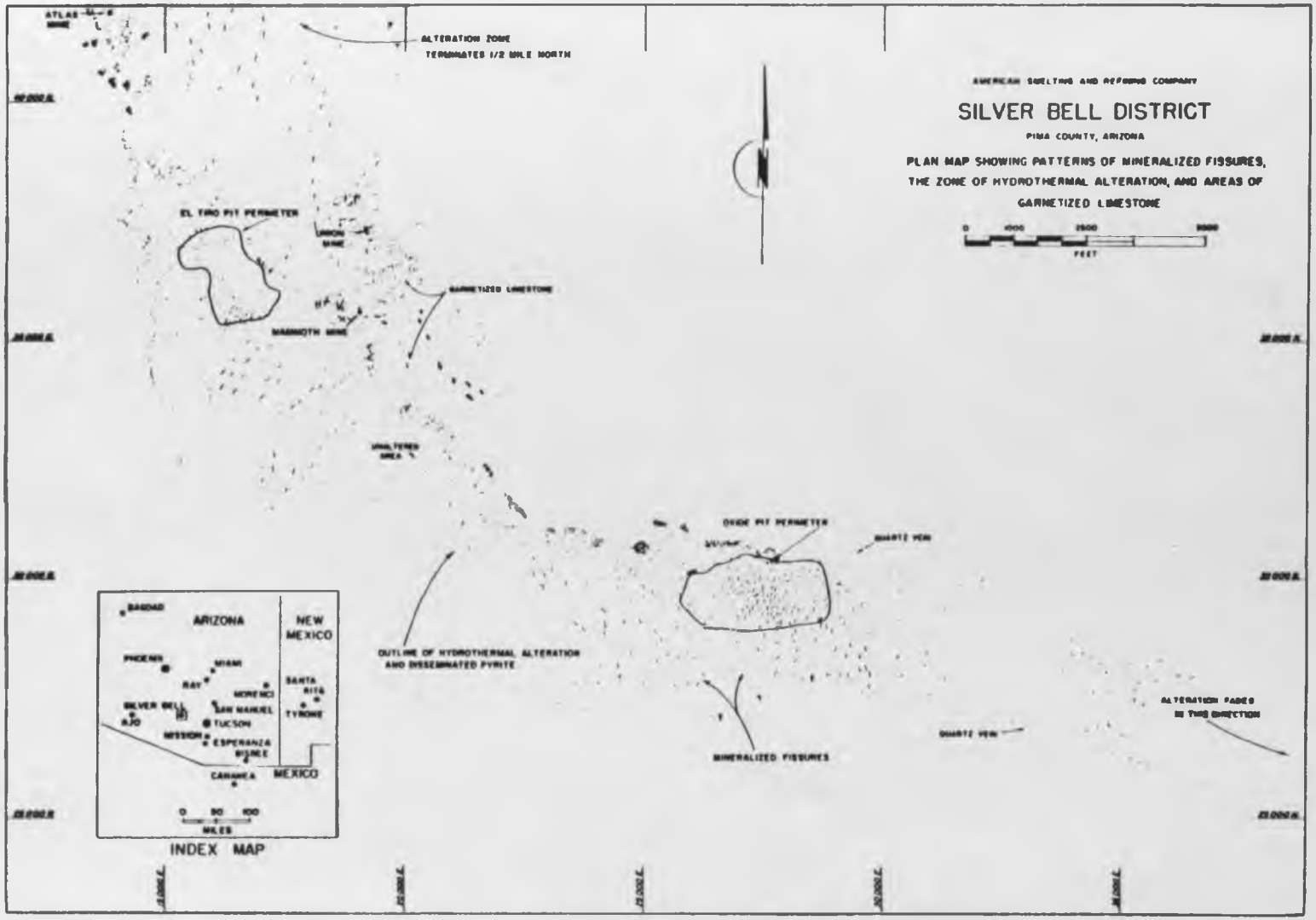

Figure 2. Location map showing Silver Bell District, and El Tiro and Oxide Pit perimeters -- From Richard and Courtright (1966).

the total sulfide content averages 5-7 volume percent (Graybeal 1982). Acid inert quartz and slightly reactive sericite, together with high concentrations of pyrite in the phyllic alteration assemblage, makes the alaskite at Silver Bell a particularly good host rock for supergene enrichment.

The enriched chalcocite blanket, inferred to be of mid-Tertiary age, is generally conformable to present surface topography. Its upper boundary can be described as a horizontal surface that once marked the transition between oxidizing and reducing conditions which probably coincided with the top of a former water table. The distribution of ore grade copper mineralization is approximately uniform throughout the enriched blanket and does not reflect the grade of the underlying hypogene mineralization (Graybeal 1982).

The drill core used in this study was from a vertical hole that penetrated the oxidized, enriched, and protore zones of an enrichment profile. The oxidized zone is 200 feet thick with an average grade of .02 percent Cu. Pyrite in this zone is replaced by iron oxide minerals goethite and hematite. The enriched zone is 350 feet thick with an average grade of .63 percent Cu. Chalcocite and pyrite are the dominant sulfides. The protore zone continues from the base of the enriched zone to the bottom of the drill hole with hypogene mineralization grades that average .10 percent Cu,

with 1 percent estimated total sulfides, and a pyrite to chalcopyrite ratio of 18:1.

Thin section analyses of the drill core silicates reveals a complex pattern of supergene alteration over hypogene alteration, both of which are imposed upon a simple alaskite mineralogy. Sericite or white mice is present throughout all of the samples in a variety of habits. As part of the phyllic hypogene alteration it is closely associated with pyrite crystals in the enriched and protore zones and with pyrite remnants in the oxidized zone, the sericite is distinguished by its large (up to 20 micron) size and lath shaped crystals. A much finer grained sericite pervasively alters feldspar and groundmass in the oxidized and enriched zones of the drill hole and is probably related to the supergene event. Although it would be impossible to definitively distinguish the finer grained mica as supergene without precise stable isotope analyses (Sheppard, Nielson, and Taylor 1967), it should be noted that the very fine grained sericite habit appears only in the upper alteration zones where the effects of acid sulfate waters is the most pronounced.

A third form of sericite alteration present in the drill core samples occurs as an alteration coating on plagioclase phencrysts. Graybeal's (1982) study of the El Tiro pit notes that this alteration style is not related to rock type, sulfide type or abundance, or surface weathering,

and is not part of the phyllic assemblage. Graybeal suggests that although the age of the alteration is unknown, because of its widespread distribution it may be related to hypogene potassic or propyllitic alteration. Owing to the complex nature and variety of mica alteration present, a quantitative analysis of the amount of silicate alteration produced by supergene solutions would not yield reliable results and was not attempted in this study.

Another alteration silicate mineral prevalent in the drill hole samples is a brown poorly crystallized montmorillonite that is generally limited to feldspar phenocrysts. Graybeal (1982) points out that in the El Tiro area this alteration is not zoned away from any specific veins, and is confined to areas of higher grade chalcocite enrichment, suggesting that the alteration is supergene in origin. However, in the drill core examined, the pervasive montmorillonite alteration persists to the bottom of the hole where acid soluble minerals chlorite and calcite are present as well. If the montmorillonite was supergene in origin it could not be a product of decending acid sulphate solutions because it is stable in the presence of calcite and chlorite. The hypothesis that the montmorillonite is not stable in acid environments is further supported by the fact that in the low pH oxidized zone the montmorillonite is totally altered to kaolinite and is only stable through the enriched and protore zones. The results of this study

suggest the brown clay alteration is part of an argillic event that predates the supergene enrichment of copper.

III. X-ray Diffration Analyses.

Identification of the less that 2 micron mineral fraction of drill core sample was done by x-ray diffraction analysis. This size fraction is dominated by phyllosilicate clay minerals that, because of their small size and therefore their reactivity, are probably the best indicators of silicate chemical equilibrium through the supergene system.

Each of the twenty drill core samples was crushed in a jaw crusher and powdered using a rotating disc pulverizer. The resulting powder was sieved and the fraction passing 250 mesh recovered. Separation of the less than 2 micron fraction was accomplished by sedimentation in distilled water and calgon (sodium hexametaphosphate and sodium carbonate) to prevent flocculation. The less than 250 mesh material was placed in quart sized mason jars, agitated, and settled for a length of time (4 hours) calculated by Stokes' law for settling of spherical particles that allowed recovery of the clay size particles. The upper 5 cm of water and its suspended solids was recovered by pipette and was then centrifuged, the supernatant liquid discarded and the remaining slurry was deposited on a glass slide. The slides were dried overnight and then x-rayed using a Siemens D500 diffractometer and goniometer equipped

with a graphite crystal monochrometer. The slides were scanned from 3°20 to 50°20 at 1°20 per minute, and peaks were reproduced on a Kompensograph-XT chart recorder.

The phyllosilicate clay minerals have a platy habit and therefore settle from the slurry in an oriented manner and in a uniformly thick layer. An oriented mount will give the first (001) basal spacings of well crystalizied clay minerals. The d spacings obtained from the initial diffractogram are compared to standard minerals and the unknowns are identified. Auxillary treatments for the identification of clay minerals are glycolation and heating, which cause measurable, distinctive expansion or contraction of the c latice dimension. With prolonged heating the crystalline structures of minerals such as kaolinite break down and the mineral becomes amorphous.

After the initial x-ray diffraction scan the slides were glycolated for four hours at 50°C, and x-rayed at the same scan rate and degree interval. Smectites are identified by their characteristic swelling on glycolation from a d spacing of about 15Å to 17Å. (Chlorite or micas will will not expand on glycolation unless interlayered with montmorillonite.)

Finally the slides were heated in a furnace at 600°C for one hour resulting in the destruction of kaolinite crystallinity and intensification of the 14Å chlorite reflection, allowing identification of chlorite. The glass

slides were supported in the furnace by flat fire bricks to prevent warping of the glass at high temperatures. The slides were slowly cooled and immediately reanalyzed.

There are four clay minerals present in the drill core that were identified by x-ray diffraction analysis -- kaolinite, sericite, montmorillonite, and chlorite. There is a slight hump to the low angle side of the 10Å mica peak in many of the samples which indicates the presence of some mixed layer clays.

Figure 3 plots each of the clay types as percent of total clay size fraction in a particular sample versus depth of the drill hole. The relative abundances were calculated from measurements of basal peak heights of the dominant (001) reflection that characterizies the particular clay of interest. Chlorite was not considered as part of the total clay size fraction because it is present only in minor amounts at the base of the enriched zone. Also plotted in Figure 3 is copper grade that delineates the oxidized, enriched, and the protore zones. In addition to their sample numbers, individual sample clusters or groups are also numbered in Figure 3 for future reference.

Sericite is the dominant clay mineral throughout the drill hole. Kaolinite is present in significant amounts in the upper oxidized zone but is trivial in the enriched and protore zones where montmorillonite becomes important, while in the oxidized zone no montmorillonite exists. The

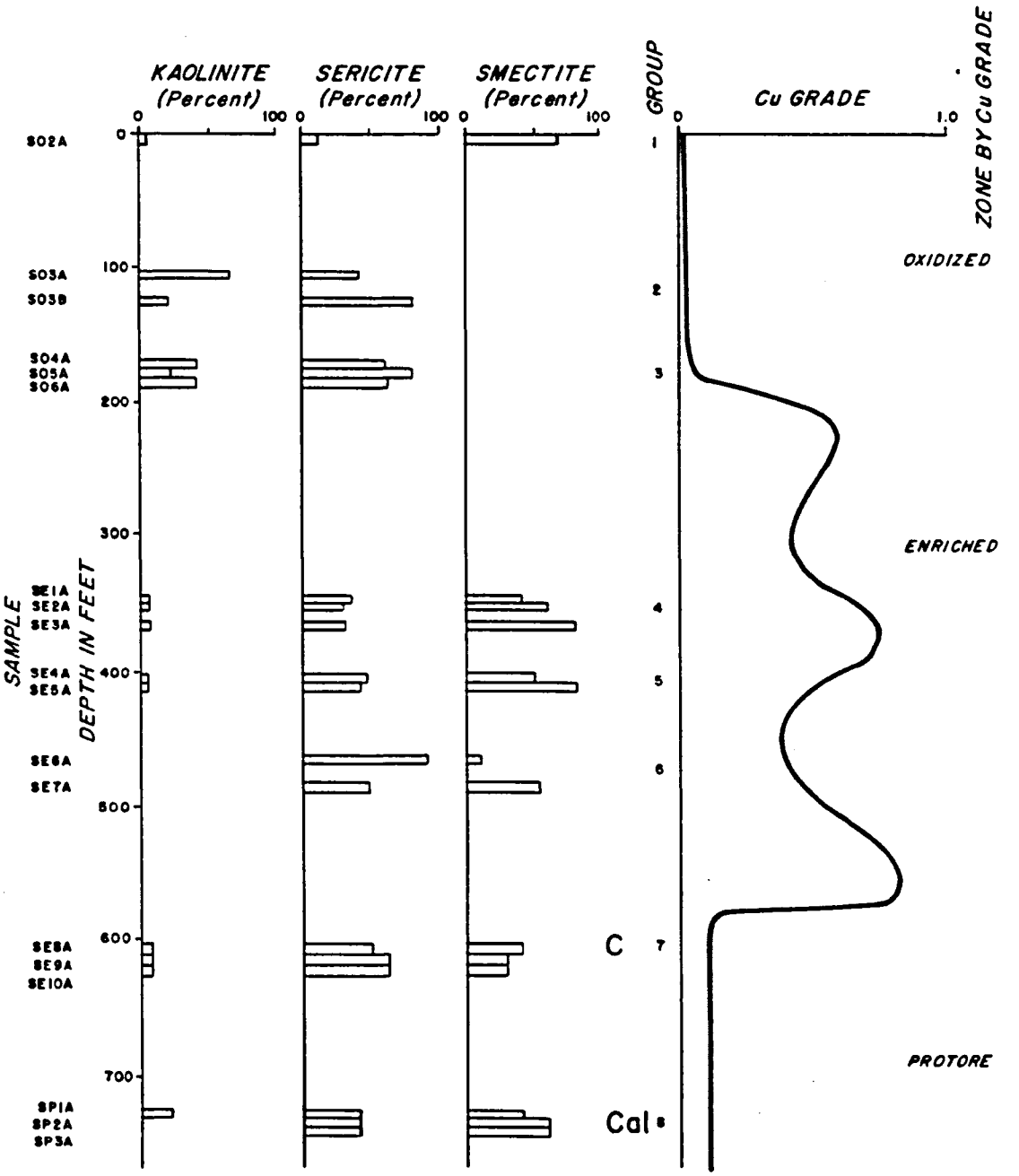

Figure 3. Relative percent of the mineral of interest to total clay size fraction with copper grade versus depth. C - marks chlorite appearance, Cal - marks calcite appearance.

lack of smectite minerals in the oxidized zone and the predominance rather of kaolinite implies that the montmorillonite has been chemically altered to kaolinite by the supergene process and the fact that the switch occurs at the oxidized-enriched interface suggests that the alteration reaction stops when the same conditions that stabilize metal sulfides are realized.

Chlorite is present in the #7 group samples, which lie just at the base of the enriched zone. No chlorite peaks were detected above or below this group. Although the chlorite might then be authigenic, definitive single crystal x-ray photographs that would distinguish high temperature from low temperature chlorite were not possible with the drill core used in this study. It is important to note, however, that it is just below the enriched zone that chlorite becomes stable.

Anderson (1982) describes supergene alteration that extends into the protore zone in many copper sulfide deposits. The presence of chlorite and biotite serves as a measure of the depth to which supergene acid attack is effective because these minerals are stable only under neutral to alkaline conditions. The appearance of chlorite at 600+ feet and calcite at 700+ feet would mark the limit of sulfide alteration in the drill core area of Silver Bell Mine.

The coarse fraction of the powdered core sample was analyzed by x-ray diffraction for minerals other than the clays. The sample was reagitated after the less than 2 micron fraction was removed and allowed to settle for 30 seconds; the suspended solids and solution were siphoned from the jar. The settled portion was then deposited in a slurry on glass slides, allowed to dry and x-rayed in the manner previously described. Quartz, orthoclase, and albite were the only new minerals identified. In samples from the oxidized zone and enriched zone, sericite was part of the coarse size fraction. No jarosite or alunite was detected, thus a comparison to Bladh's (1978) sulfide-silicate theoretical data was not possible.

IV. Electron Microprobe Analyses.

The next step in describing silicate-solution alteration reactions is an analysis of silicate mineral chemistry as it changes with depth in the system. If equilibrium can be assumed between minerals of the clay size fraction and the last reacting solution, knowledge of clay mineral chemistry can lead to an understanding of how the solution chemistry changes, and how these changes can effect metal deposition.

Electron microprobe analysis of the phyllosilicate minerals allows in situ collection of chemical data. Thin sections cut from drill core samples were specially polished

to eliminate surface roughness to insure low beam scatter. Analysis points were predetermined by thin section examination under the petrographic microscope. Black and white photographs were taken of each thin section and were used as maps for locating points analyzed by microprobe. Certain minerals in slides from the enriched zone were found to exsolve solution bubbles under the electron beam; this exsolution interfered with the acquisition of reliable results. All the thin sections were then heated to 50°C for 1 hour under vacuum to remove interlayer water without destroying crystal structure. The slides were kept in a desiccator until microprobe analysis was complete.

Normal wavelength dispersive system (WDS) analyses were made with an accelerating voltage of 15 Kv, a specimen current of 25 nanoamps, and an electron beam diameter between 10-30 microns. Concentrations were calculated using simple silicate minerals as standards and corrective calculations carried out using the Bence-Albee correction procedure. Volitalization effects are minimized under the current and voltage used in this study. This was verified by test count runs on potassium and sodium concentrations of sericite minerals in some sample thin sections. Count rates (counts/second) after 60 second intervals were found to vary within only four percent of count rates made at an initial 10 second count interval. The counting intervals used for the alkali metals in the chemical analysis of the

clays were 50 seconds, thus accurate concentration analysis could be obtained with minimum volitalization. All concentration ratio values of the major mineral forming elements were determined within 0.5 percent error between the unknown and the standard peak counts.

Over 280 chemical analyses were made of individual minerals in 21 thin sections. Feldspars that were analyzed showed no significant change in composition with depth (Table 1). Only ten kaolinite analyses were collected, all from the oxidized zone and only about ten chlorite minerals were analyzed, all from the interface between the enriched and the protore zone. The remaining analyses were predominantly of micas. The mica clay minerals were the only silicates that exhibited compositional changes with depth. Only those illite-sericite mineral analyses whose sum of the oxide components was between 93.5 and 97 percent, which allows for 6.5-3 percent H_2O^+ in the mineral structures, were finally used in this study. These analyses have been recalculated assuming $Fe^{2+}/(Fe^{2+} + Fe^{3+}) = .865 = Fe^{3+}/Fe$ total, an average value for illite tabulated by Weaver and Pollard (1973). The stoichiometry was then evaluated for an ideal mica composition requiring that the sum of positive charge equals 22.0. An ideal tetrahedral occupancy of 4.00 is assumed to be filled by silica and alumina, with the excess alumina filling the octahedral site along with

Table 1. Results of electron microprobe analyses of feldspars-stoichiometries (on 8 oxygens).

Group	Elements							Percent	Group
	Na	K	Ca	Al	Si	Mg	Fe		
1	0.04	0.96	0.00	1.02	2.96	0.00	0.00	98.07	1
	0.11	0.90	0.00	1.01	2.99	0.00	0.00	97.98	
	0.03	0.96	0.00	1.03	2.98	0.00	0.00	98.83	
2	0.91	0.01	0.02	1.07	2.95	0.00	0.00	99.30	2
	0.92	0.01	0.01	1.07	2.95	0.00	0.01	99.51	
	0.02	0.97	0.00	1.02	2.99	0.00	0.00	98.92	
	0.13	0.80	0.00	0.97	3.04	0.00	0.00	100.25	
4	0.53	0.93	0.00	1.03	2.98	0.00	0.00	97.92	4
	0.94	0.01	0.01	1.04	2.98	0.00	0.00	99.68	
	0.92	0.03	0.02	1.06	2.96	0.00	0.00	99.20	
5	0.84	0.07	0.00	1.09	2.94	0.02	0.01	97.95	5
	0.66	0.30	0.02	1.01	2.99	0.00	0.00	99.46	
	0.95	0.01	0.01	1.03	2.98	0.00	0.00	99.96	
	0.19	0.82	0.00	1.02	2.98	0.00	0.00	100.49	
	0.95	0.01	0.03	1.08	2.94	0.00	0.00	100.33	
	0.91	0.04	0.01	1.14	2.89	0.02	0.01	100.79	
6	0.96	0.02	0.00	1.05	2.97	0.00	0.00	103.47	6
	0.02	0.98	0.00	1.04	2.97	0.00	0.00	99.69	
	0.91	0.01	0.06	1.11	2.91	0.00	0.00	101.78	
	0.88	0.01	0.06	1.11	2.92	0.00	0.00	102.56	
7	0.84	0.08	0.02	1.08	2.95	0.01	0.00	99.72	7
	0.85	0.04	0.06	1.10	2.92	0.00	0.00	99.55	
	0.18	0.82	0.00	1.01	2.99	0.00	0.00	98.69	
	0.91	0.05	0.02	1.10	2.92	0.00	0.00	97.16	
8	0.05	0.97	0.00	1.00	2.99	0.00	0.01	98.81	8
	0.07	0.95	0.00	1.00	3.00	0.00	0.00	99.01	
	0.89	0.03	0.03	1.03	2.98	0.00	0.00	97.99	

Note 1:

Group	Zone
1,2	Oxidized
4,5,6	Enriched
7,8	Protore

magnesium and iron. Calcium, sodium, and potassium all fill interlayer sites.

Figures 4-6 plot stoichiometric values of the mica mineral forming cations against each other to show how chemical compositions are changing with depth in the supergene system. In all of the diagrams the mica analyses from oxidized samples cluster at the end of the line marked O, while the remaining samples generally get closer to point P as sample depth increases to the protore zone. Figure 4 plots alumina versus silica and indicates that aluminum in the micas increases and silica decreases as the effects of acid leaching becomes stronger. Figure 5 shows how total iron (Fe^{2+} + Fe^{3+}) and magnesium concentration decreases as the samples become more leached toward the oxidized zone. Figure 6 shows two examples of how leaching effects site occupancy in the mica. Figure 6a plots aluminum in the octahedral site versus the ratio of aluminum to total octahedral cations. This graph shows that the aluminum octahedral ratio approaches one and the value of octahedral aluminum approches 2.0 as the sample becomes more leached. In other words, leaching is effectively removing all cations except aluminum from the octahedral site. Similar leaching of the interlayer site is obvious from Figure 6b where the values of potassium and total interlayer cations simultaneously approach the value one from the protore to oxidized zones. It appears that local equilibrium of the mica clay

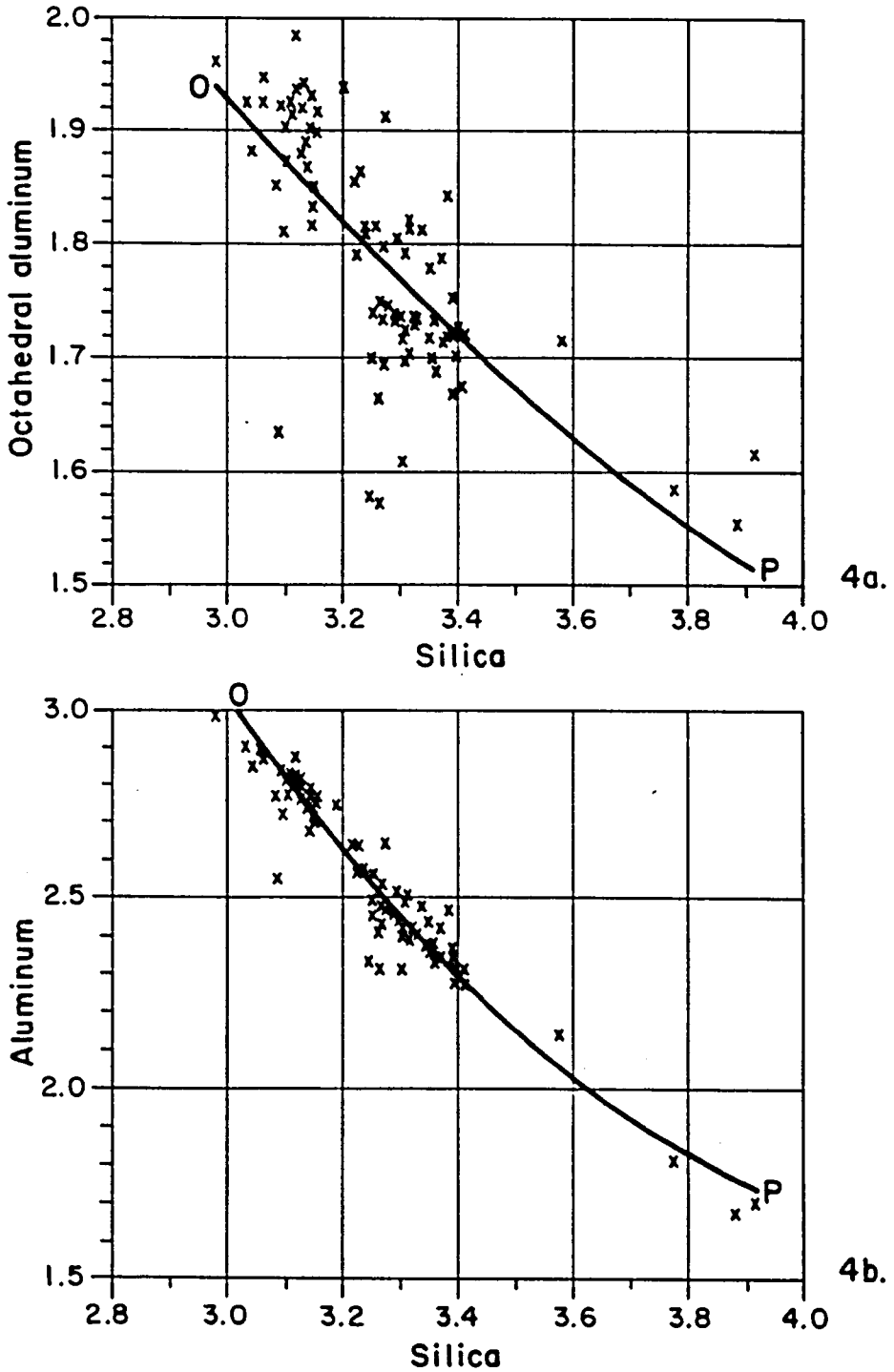

Figure 4. Chemical trends of mica minerals from the oxidized (O) to protore (P) zones. 4a plots octahedral aluminum versus silica and 4b plots total aluminum versus silica.

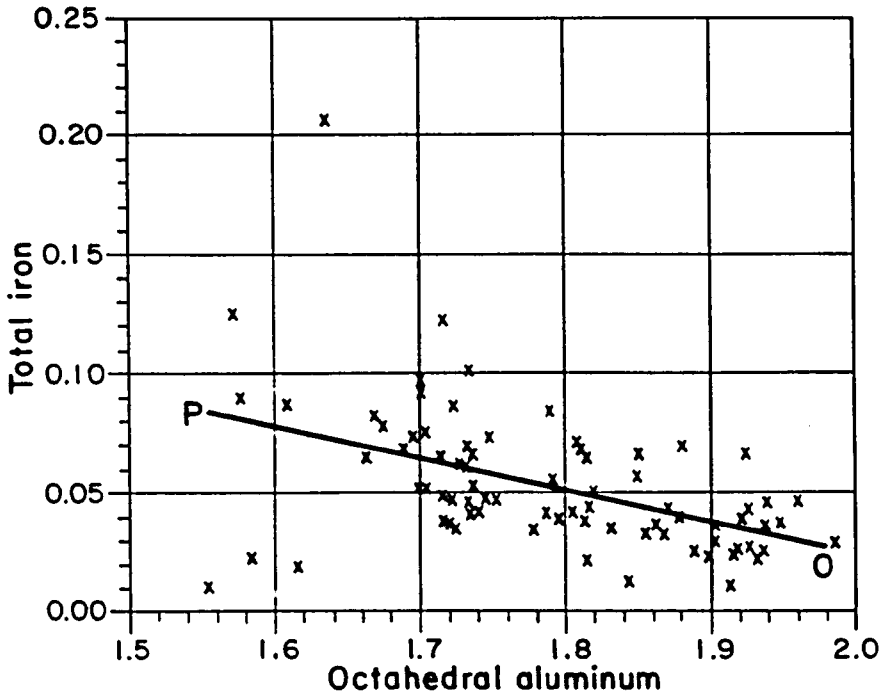

5a.

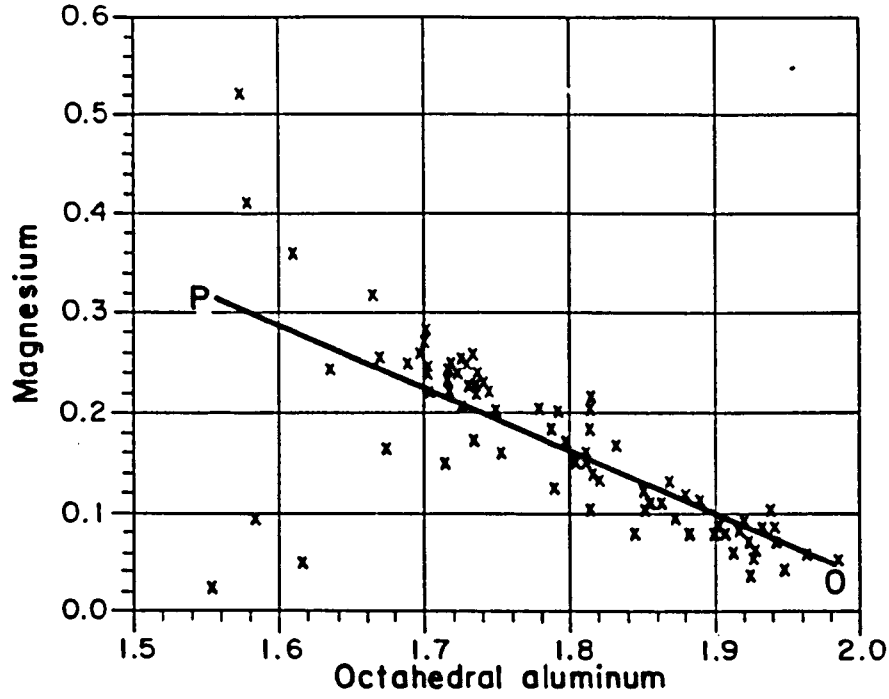

5b.

Figure 5. Chemical trends of mica minerals from the oxidized (O) to protore (P) zones. 5a plots total iron versus octahedral aluminum, 5b plots magnesium versus octahedral aluminum.

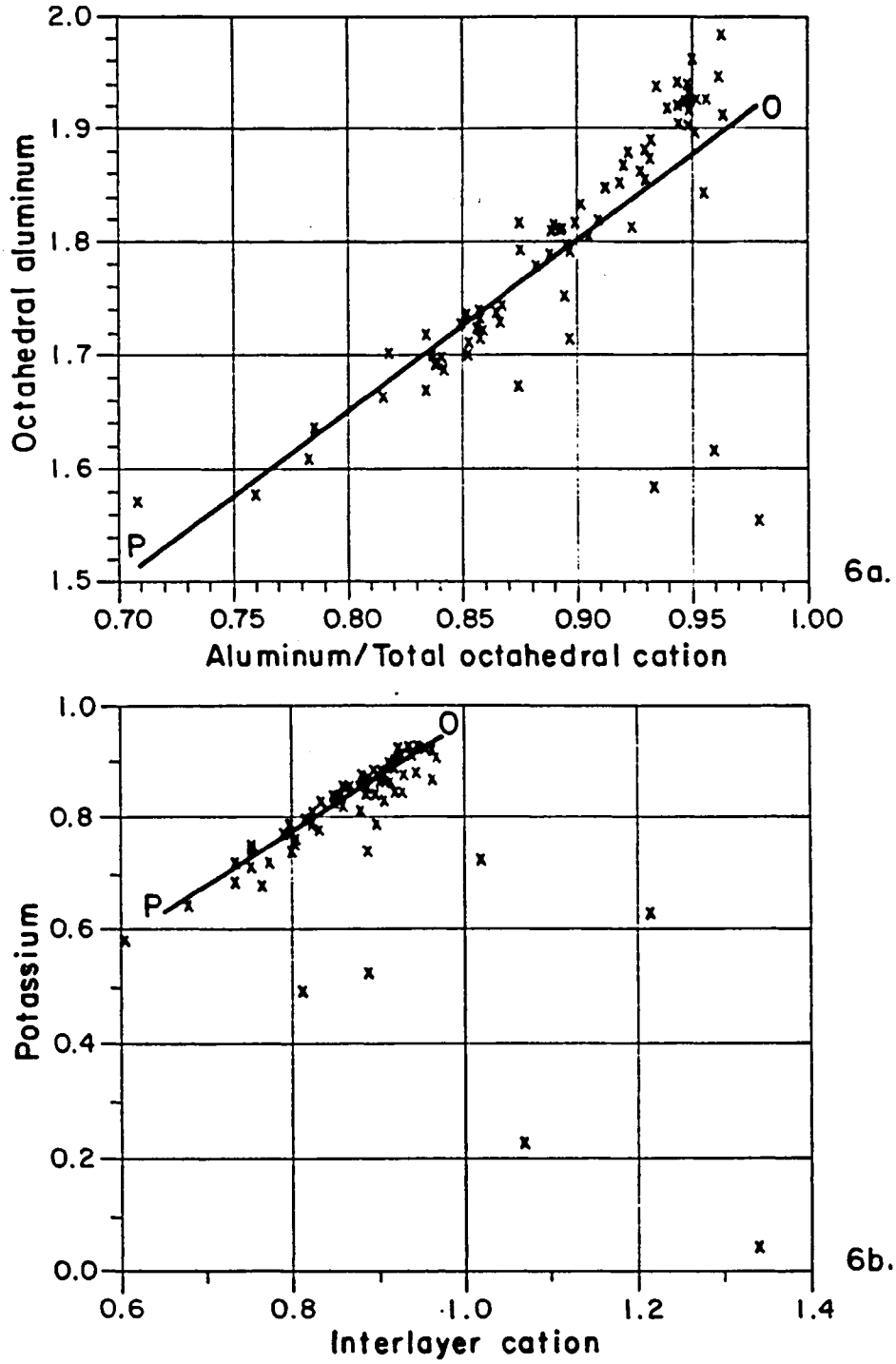

Figure 6. Chemical trends of mica minerals from the oxidized (O) to protore (P) zones. 6a plots octahedral aluminum versus the ratio of aluminum in the octahedral site to total octahedral occupancy, 6b plots potassium versus total interlayer occupancy.

minerals is reached not by complete dissolution of an unstable phase and precipitation of a stable phase but by chemical site leaching of cations from the clay structure.

Analyses of mica composition are averaged and listed in Table 2. The data reinforce compositional trends observed in Figures 4-6. Sodium and calcium are leached from the interlayer site relative to potassium. Magnesium and iron are leached from the octahedral site and silica from the tetrahedral site relative to aluminum.

Although as noted before it was not possible to petrographically distinguish between sericite minerals of hypogene or supergene origin, a sampling bias toward what is probably hypogene sericite occurs in the electron microprobe analyses. The large, lath shaped sericite crystals associated with pyrite were readily recognized under the electron probe microscope and produced the best analytical results owing to the ease with which the electron beam could be accurately focused on a single grain. Regardless of the origin of the sericite if equilibrium is assumed between the clay size grains and solution, the compositional averages probably reflect chemical trends of altered or precipitated mica minerals. The chemical data indicate that acid sulfate solutions effect sericite minerals by selective leaching of alkali and alkali earth cations from the mica without necessarily destroying the mineral structure.

Table 2. Average electron microprobe analyses of mica minerals-stoichiometries (on 11 oxygens).

Group	Elements									Group
	Na	K	Ca	AlO†	AlT*	Si	Mg	Fe^{3+}	Fe^{2+}	
1	0.06	0.91	0.00	1.86	0.91	3.10	0.10	0.05	0.01	1
2	0.05	0.81	0.00	1.89	0.87	3.13	0.10	0.04	0.01	2
3	0.01	0.84	0.00	1.74	0.70	3.30	0.21	0.06	0.01	3
4	0.01	0.82	0.00	1.73	0.63	3.37	0.28	0.05	0.01	4
5	0.02	0.84	0.00	1.74	0.69	3.31	0.21	0.06	0.01	5
6	0.03	0.83	0.01	1.77	0.73	3.27	0.19	0.05	0.01	6

†AlO - Aluminum octahedral

*AlT - Aluminum tetrahedral

Note 1: .865 = Fe^{3+}/Fe_{total}

Note 2: Number of analyses in group average

2	1
25	2
5	3
4	4
12	5
8	6
11	7
6	8

Note 3:

Group	Zone
1,2,3	Oxidized
4,5,6	Enriched
7,8	Protore

V. Whole Rock Chemical Analyses.

Whole rock chemical analyses of one representative example from each of the eight sample groups was done with x-ray flouresence spectrometry by X-ray Assay Laboratories, Ltd., Don Mills, Onatario. The results are compiled in Table 3. The whole rock analyses show losses of calcium, sodium, and silica; and relative gains of aluminum and iron in the oxidized zone. There is also a distinct increase in the amount of material lost on ignition in the oxidized zone presumed to be OH from the hydration of silicate minerals that commonly accompanies the weathering process.

For comparison whole rock analyses of cap rock and ore from three other deposits are listed in Table 4. Generally the same chemical losses of calcium, sodium, magnesium, and silica; and relative gains of H_2O^+, aluminum, and iron as are present at Silver Bell occur in rocks of these other deposits.

The prevailing effects of supergene reactions on silicate host rock is the leaching of the alkali, alkali-earth, and silica cations into solution. This process is obvious not only on a whole rock scale but also in individual silicate crystals. The resulting changes that these reactions cause in solution compositions may be found in waters presently circulating through enriched sulfide deposits.

Table 3. Whole Rock Chemical Analyses of Silver Bell Samples.

Group	Elements									Sum	Group
	SiO_2	Al_2O_3	CaO	MgO	Na_2O	K_2O	Fe_2O_3	FeO	LOI†		
1	73.8	13.3	0.13	0.31	1.04	6.06	0.43	1.70	2.39	99.4	1
2	73.4	14.2	0.10	0.27	1.28	5.79	0.72	0.72	3.00	99.8	2
3	76.7	12.4	0.09	0.21	1.74	6.57	0.45	0.30	1.54	100.2	3
4	71.9	13.9	0.13	0.26	2.25	6.61	0.49	0.49	2.08	98.4	4
5	74.2	12.3	0.16	0.20	2.33	6.37	0.53	0.80	1.54	98.7	5
6	72.2	13.5	0.22	0.24	2.83	6.17	0.31	1.24	1.62	98.5	6
7	79.4	9.87	0.47	0.20	1.84	5.42	0.44	0.44	1.00	99.3	7
8	75.4	11.6	0.68	0.28	1.56	7.42	0.34	0.34	1.54	99.3	8

†LOI = Loss on ignition

Note 1:

Group	Zone
1,2,3	Oxidized
4,5,6	Enriched
7,8	Protore

Note 2: Sum value includes trace oxide analyses not reported here.

Table 4. Whole Rock Analyses of cap rock and ore rock from sulfide rich deposits.

Component	Sample Number					
	1a	1b	2a	2b	3a	3b
SiO_2	22.44	9.95	56.70	50.55	66.83	68.30
Al_2O_3	2.93	1.57	19.35	19.93	15.92	17.41
Fe_2O_3	33.43	49.9	4.20	10.57	2.36	3.80
FeO	---	---	---	---	.92	.15
MgO	3.15	---	.37	.12	.64	.83
CaO	8.28	.35	---	---	.13	.04
Na_2O	---	---	13.97	12.13	.51	.53
K_2O	---	---			5.75	5.71
H_2O	0.00	15.40	.50	3.05	2.56	2.59

Notes:

1a=primary ore, 1b=cap rock - from Mary Mine; Ducktown, TN Emmons (1917) p. 132.

2a=primary ore, 2b=cap rock - from Moose Mine; Colorado Emmons (1917) p. 136.

3a=primary ore, 3b=cap rock - from Miami Mine; Ransome (1919) p. 165.

--- = Not analyzed for.

VI. Water Analyses.

Water samples were collected from Silver Bell mine from four separate sources and were analyzed at the University of Arizona Soil Testing Laboratory. The results are tabulated in Table 5. SBW-1 was collected from a natural seep from within the El Tiro pit. The extremely high iron and sulfate may be due to contamination by outflow waters from the solution mining leach pit at Silver Bell. SBW-2 was collected from solution entering the leach pit originating from sulfuric acid flooded copper-sulfide bearing tailings piles. SBW-3 was collected from water coming out of the leach pit after it had deposited its copper by replacement of iron from scrap metal. SBW-4 was collected from a pseudo-lake formed in the bottom of the El Tiro pit. Noteworthy are the high alkali-earth, sulfate, aluminum, and iron values of these waters.

The waters were filtered before analysis to recover the suspended solids from solution. The recovered material was identified by x-ray diffraction analysis, but only SBW-1 contained crystalline minerals. Minerals identified in SBW-1 were kaolinite, illite, microcline, albite, quartz, and jarosite.

SBW-3 with its high iron content, precipitated crystal iron hydroxides during laboratory analysis causing the lab determined pH to drop lower than the field determined value. The laboratory analysis of this sample showed

Table 5. Five water analyses in ppm from Silver Bell Mine.

Type	Sample Number	Elements										Sample Number
		pH	Mg	SO_4	Cu	Al	SiO_2	Ca	Fe	K	Na	
mine seep	SBW-1	3.2	300	13,683	5,220	397	144	461	891	9	100	SBW-1
leach	SBW-2	3.0	1,415	17,494	886	1,620	146	541	104	1	28	SBW-2
post-leach	SBW-3	3.7	1,383	15,557	12	260	139	542	843	2	28	SBW-3
pit lake	SBW-4	6.7	117	1,296	---	31	55	481	---	6	53	SBW-4

it was not electrically balanced possibly due to the presence of some components as colloidal particles.

Of all four water samples, SBW-2 seems to be the best example of a solution that would be the result of acid sulfate attack upon copper-sulfide rich silicate rock. The analyses of SBW-2 are therefore used in all subsequent calculations as a typical solution in Silver Bell supergene processes.

For comparison, water analyses from ten other copper mines are compiled in Table 6. Waters were chosen that exhibited high sulfate values similar to the Silver Bell waters. These examples and the Silver Bell waters show high values of alkali-earth cations that are consistent with the chemical changes observed in the rock analysis. The lack of silica or alkalis in the water is noteworthy because these elements also showed losses in the rock analyses; however their presence and abundance may be controlled by the precipitation of some supergene minerals. Aluminum is unexpectedly high but an increased solubility of aluminum in sulfate rich solution is noted by Millott (1970). All the alkali, alkali-earth, silica, and aluminum cations in these typical mine waters are produced by silicate mineral reactions. It is obvious that the weathering of silicate minerals has a direct effect upon the composition of solutions responsible for the deposition of enriched copper deposits.

Table 6. Sulfacte rich water analyses from copper-sulfide mines (in ppm).

Component	Sample Number									
	1	2	3	4	5	6	7	8	9	10
SO_4	71,053	2,672	6,664	2,068	5,064	1,419	4,457	3,898	1,335	29,325
SiO_2	67	48	56	79	76	28	56	40	20	44
Alkali	48	52	42	13	---	170	198	97	14	38
Ca	307	133	68	238	436	319	753	239	277	194
Mg	149	62	41	63	61	36	86	82	54	165
Al	85	84	433	165	---	16	22	44	9	1,550
Cu	45,633	59	312	41	1,659	---	60	122	28	718

Analyses from Emmons (1917) p. 87.

1. Mountain View Mine; Butte, MT
2. St. Lawrence Mine; Butte, MT
3. Burra Burra Mine; Ducktown, TN
4. East Tennesse Mine; Ducktown, TN
5-9. Capote Mine; Cananea, Mexico
300, 400, 900 foot levels pumped water, concentrator water respectively.

Analyses by University of Arizona Soil Testing Laboratory

10. Mineral Park Mine; Kingman, AZ
from a seep at the base of tailings.

CHAPTER 3

DISCUSSION AND CALCULATIONS

I. Silicate Weathering Reactions.

The results of acid sulfate solution reaction with silicate minerals can be described by detailed chemical analysis of the reaction products. Knowledge of the product chemistry leads to an understanding of how these reactions may exert limitations upon copper enrichment.

The octahedral and tetrahedral site charge deficiencies were calculated from group mineral averages (Table 2) and plotted as originally done by Hower and Mowatt (1966) on a triangular plot of the system muscovite-celadonite-pyrophyllite (Figure 7). Mica minerals can be described by the solid solution of these end member components. Octahedral site exchange can be described by solid solution between muscovite and celadonite, and tetrahedral site exchange can be described by solid solution between muscovite and pyrophyllite.

The Silver Bell minerals in Figure 7 tend to approach an ideal muscovite composition in the strongly leached oxidized zone. All cations except aluminum are leached from the octahedral site, all cations except

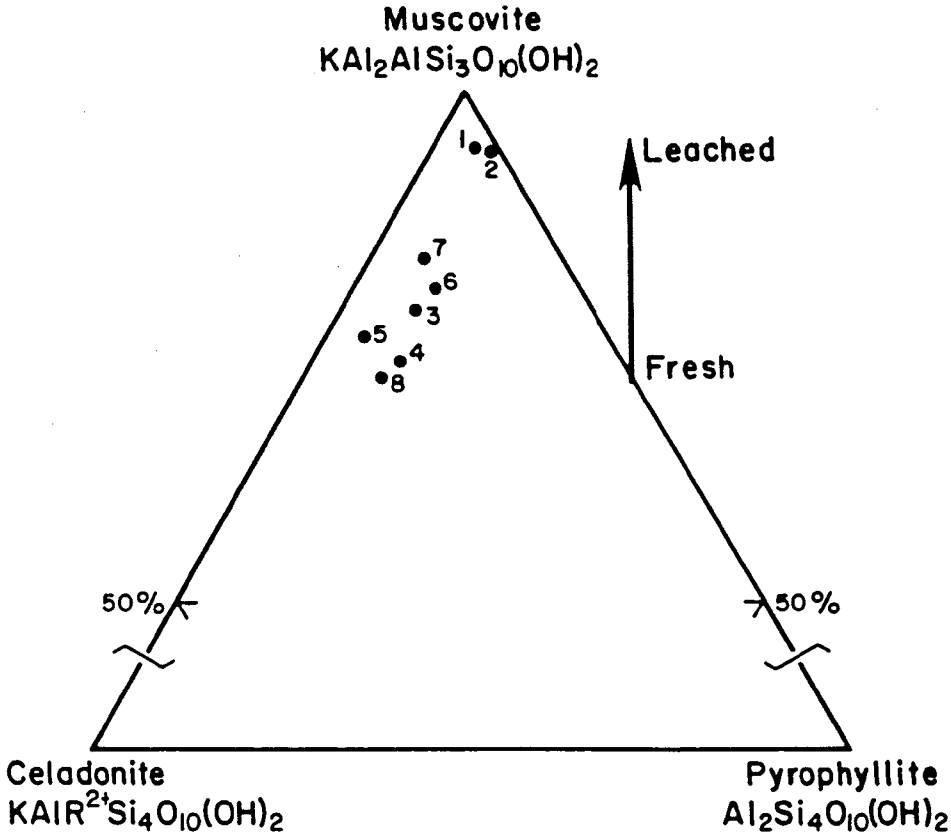

Figure 7. Oxidizied (1,2,3), enriched (4,5,6), and protore (7,8) average chemical analyses of mica minerals in the muscovite-celadonite-pyrophyllite system.

potassium are leached from the interlayer site, and silica in excess of three atoms is leached from the tetrahedral site. The question of whether the mica analyzed in the oxidized zone is hypogene or supergene is irrelevant if equilibrium of the phyllosilicate clay size minerals is assumed.

From the mineral trends identified by x-ray diffraction (Figure 3) and the chemical trends obvious from microprobe analyses (Figure 7) the following reactions can be written that describe silicate weathering in the supergene system (eqs. 3-6). These reactions release cations

3) $2KAlSi_3O_8 + 2H^+ + H_2O = Al_2Si_2O_5(OH)_4 + 2K^+ + 4SiO_2$

4) $3KAlMgSi_4O_{10}(OH)_2 + 2H^+ + 6H^+ = KAl_2AlSi_3O_{10}(OH)_2 + 3Mg^{2+} + 9SiO_2 + 2K^+ + 6H_2O$

5) $Ca_{.33}Mg_{.66}Al_{3.34}Si_8O_{20}(OH)_4 \cdot nH_2O + 1.98H^+ + .32H_2O = 1.67Al_2Si_2O_5(OH)_4 + .33Ca^{2+} + .66Mg^{2+} + 4.66SiO_2$

6) $Al_2Si_2O_5(OH)_4 + 6H^+ = 2SiO_2 + 2Al^{2+} + 5H_2O$

K^+, Mg^{2+}, Ca^{2+}, and Al^{3+} into solution while they consume hydrogen ion. The release of cations is reflected in water composition analyses (Tables 5 and 6). The consumption of

hydrogen is obvious in mineralogical changes with depth in the drill hole. The silicate minerals function in the supergene system in two ways, as a cation contributor and as a hydrogen consumer, these chemical influences can have a definite effect on copper enrichment.

II. Complex Competition.

Cations in an aqueous medium react with available bases in order to improve the stability of electrons in their outer shell. Metal ions can react to achieve such stabilization without the formation of precipitates by forming metal coordination complexes with anions or negatively charged molecules called ligands. The number of ligands that can coordinate with a particular metal cation depends on how many ligands can arrange themselves around the central cation which is basically a function of size. In solution, free metal cations are continuously searching for ligands to form stable complexes. Actually free cations are coordinated by polarized water molecules and coordination reactions are really exchange reactions between a preferred ligand and the water molecule. In concentrated solutions the metal cations will compete for the preferred ligand and the resulting degrees to which the cations are coordinated is determined by complex stability constants. The competition for ligands is of fundamental importance when describing the effects of silicate reaction on metal

enrichment because copper metal ions and silicate related cations simultaneously compete for sulfate ligand in solution.

Complex stability can be described by simple equilibrium relationships (Freiser and Fernando 1979). Ratios of concentrations of metal complex species of total metal concentrations (C_m) are defined by a term designated by β:

$$7)\ \beta_0 = (M)/C_m$$

$$8)\ \beta_1 = (ML)/C_m$$

$$9)\ \beta_2 = (ML_n)/C_m$$

where (M) represents metal ion activity, (L) represents ligand activity, and (ML_n) represents the complex species activity. Using simple algebra and by defining $k_n = (ML_n)/(M*L_{n-1})*(L)$.

$$10)\ \beta_0 = \frac{1}{1 + k_1 + k_1*k_2*(L)^2 + \cdots + k_1*k_2*\cdots*k_n(L)^n}$$

$$11)\ \beta_1 = \frac{k_1(L)}{1 + k_1 + k_1*k_2*(L)^2 + \cdots + k_1*k_2*\cdots*k_n(L)^n}$$

$$12)\ \beta_n = \frac{k_1*k_2*\cdots k_n*(L)^n}{1 + k_1 + k_1*k_2*(L)^2 + \ldots + k_1*k_2*\cdots*k_n(L)^n}$$

These equations are very useful in calculating concentrations of any metal complex species provided the equilibrium concentration of the ligand is known.

Figure 8 plots the concentration of metal complex species in terms of $Log\beta_n C_m$ versus sulfate ligand for metal concentrations of SBW-2. For any particular species the relative amounts of free to complex coordinated ligand can be read directly from the diagram. At the stability constant value of ligand (Sillen 1964) the concentration of the free or hydrated cation equals the concentration of the complex species, while at lower ligand concentrations free metal is the dominant species and at higher ligand concentrations a metal complex will be the most stable. Aluminum coordinates with two sulfate ligands and, therefore has two different complex stability constants. The value of SO_4^{2-} in SBW-2 is $10^{-.74}$ molarity. In Figure 8 at this value of sulfate concentration $Mg(SO_4)^0$ is the dominant sulfate species in solution, in effect, because of the high concentration of magnesium and because of the stability of the magnesium-sulfate complex. In SBW-2 as Figure 8 indicates, sulfate complexes more strongly with magnesium than with either aluminum or copper.

The effects of complex competition between cations in any solution can be described by equations that take into account the masking capabilities of side reactions. Because copper travels in oxidized sulfide systems predominantly as $CuSO_4^0$ the reaction of copper ion to copper sulfate will be the main reaction of interest. The equilibrium expression for the reaction is:

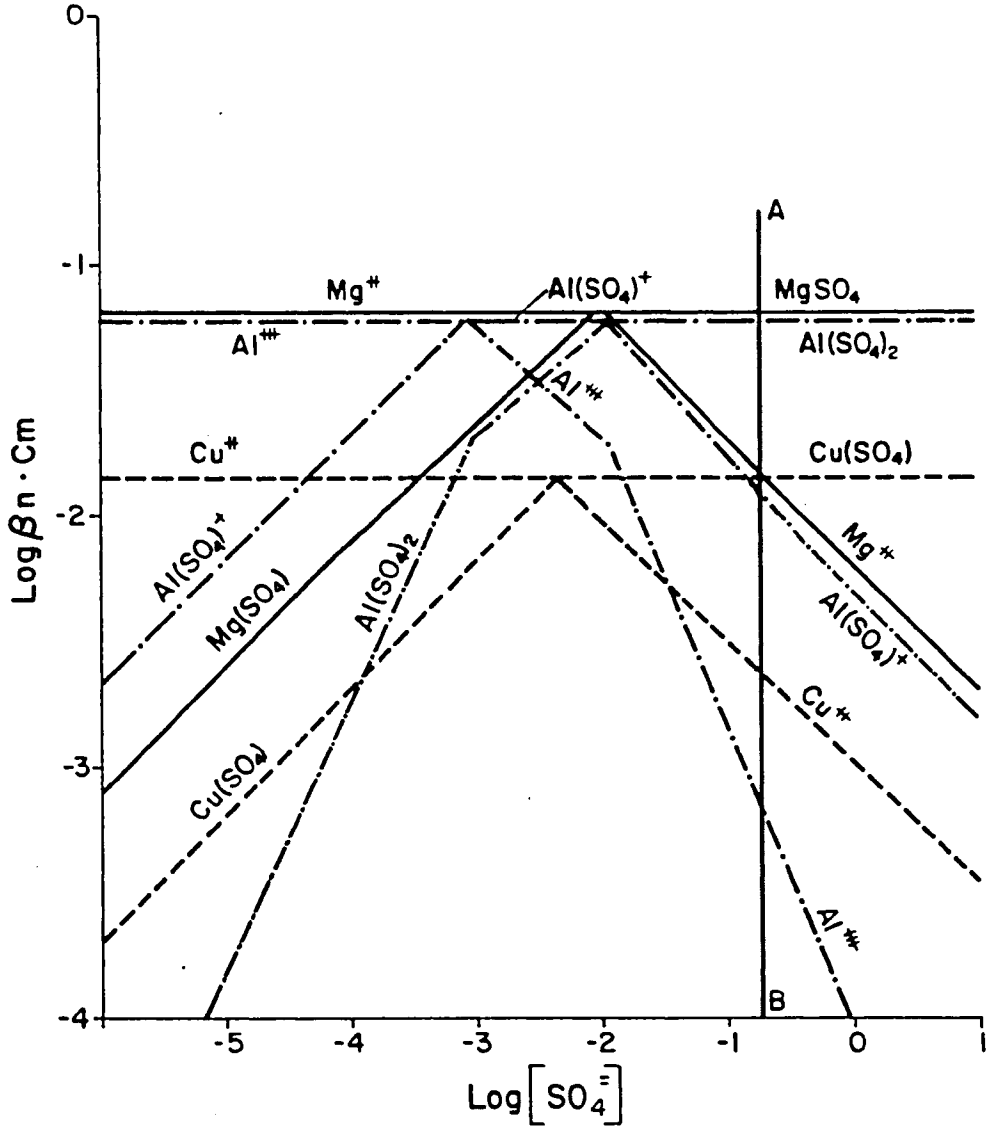

Figure 8. Concentration of metal-sulfate complexes versus sulfate concentration for SBW-2. Line A-B marks sulfate concentration of analyzed sulfate in SBW-2.

13) $\log k = \log(CuSO_4^0)/(Cu^{2+})(SO_4^{2-}) = 2.35$

All equilibrium values are from Sillen and Martell (1964). Side reactions effect the main reaction by competing for

14) $Cu^{2+} + nOH^- = CuOH_n^{(2-n)}$

15) $MSO_4^0 = M^{2+} + SO_4^{2-}$

16) $HSO_4^- = H^+ + SO_4^{2-}$

ligand or copper ions. These reactions are represented in the main reaction by α and β values.

17) $$k = \frac{\beta_{CuSO_4}(CuSO_4^0)}{\beta_{Cu}(Cu^{2+}) * \alpha_{SO_4}(SO_4^{2-})}$$

An α describes a dissociation fraction which is the ratio of the concentration of any species to the sum of the concentration of all species. α differs from β in that β is an association value. A conditional equilibrium constant k' can be derived for the main reaction.

18) $$k' = \frac{k\beta_{Cu}\,\alpha_{SO_4}}{\beta_{CuSO_4^0}} = \frac{(CuSO_4^0)}{(Cu^{2+}) * (SO_4^{2-})}$$

In a simple supergene system the only side reaction affecting copper cation is equation 17, the β value for this reaction is:

19) $$\beta_{Cu} = \frac{[M]}{C_m} = \frac{Cu^{++}}{Cu^{++} + Cu(OH)^+ + Cu(OH)_2^0 + Cu(OH)_3^- + Cu(OH)_4^{2-}}$$

$$20)\quad \beta_{Cu} = \frac{1}{1 + k_1(OH) + k_1k_2(OH)^3 + k_1k_2k_3(OH)^3 + k_1k_2k_3k_4(OH)^4}$$

if pH is known, the value of β_{Cu} can be determined. There are no side reactions involving $CuSO_4^0$, so $\beta CuSO_4^0$ is equal to zero. There are two side reactions that effect SO_4^{2-}, these are described in equations 15 and 16. α for equation 16, where C_L is the total concentration of ligand is:

$$21)\quad \alpha_1 = \frac{(SO_4)}{C_L} = \frac{k_1}{H + k_1}$$

and α_1 can be calculated if pH is known. For equation 15, depending on the metal (M) involved α_n can be calculated if the metal concentration is known. For metals that complex in a 1:1 ratio with ligand such as magnesium or calcium, α_1 equals:

$$22)\quad \alpha_1 = \frac{(M)}{C_m} = \frac{k_1}{M + k_1}$$

For metals that complex in a 2:1 ratio with ligand like aluminum, α_2 equals:

$$23)\quad \alpha_2 = \frac{(M)}{C_m} = \frac{k_1k_2}{M^2 + Mk_1 + k_1k_2}$$

The combined effect of equations 15 and 16 on sulfate ligand concentration is defined by:

$$24)\quad \frac{1}{\alpha SO_4^{2-}} = \Sigma \frac{1}{\alpha(x)L} - (n'^{-1})$$

$$25)\quad \frac{1}{\alpha SO_4^{2-}} = \frac{1}{\alpha HSO_4^+} + \frac{1}{\alpha MgSO_4^0} + \frac{1}{\alpha CaSO_4^0} + \frac{1}{\alpha AlSO_4^0} - 3$$

where n' equals the number of accessory metals considered.

At low pH values typical of the leached zone the effects of equation 14 are negligible so that only significant masking is described by $\alpha\ SO_4^{2-}$. The conditional constant becomes:

$$26)\ k' = k * \alpha SO_4^{2-}$$

and can be calculated if pH and concentration values of the competing metal cations are known. A pH of 3.0 is chosen as a representative value of acidity in the leached zone. Figures 9a-11a illustrate how the conditional constant changes as concentration of the metals Mg^{2+}, Ca^{2+}, or Al^{3+} changes. The value of k' decreases as the concentration of metal increases, however the amount of copper that exists as copper sulfate in solution remains a function of the sulfate activity in solution. Figures 9b-11b plot the $CuSO_4^0/Cu^{2+}$ ratio versus sulfate activity with various metal concentration contours. It is obvious that at high metal values the copper in solution as copper sulfate is low unless there is a high sulfate concentration to minimize the complex competition.

The presence of sulfate-seeking cations in solution in addition to copper has the effect of forcing copper to its free ion or hydrated state. If free copper is in excess in solution, supergene copper minerals such as cuprite, chalcanthite, or native copper will approach saturation

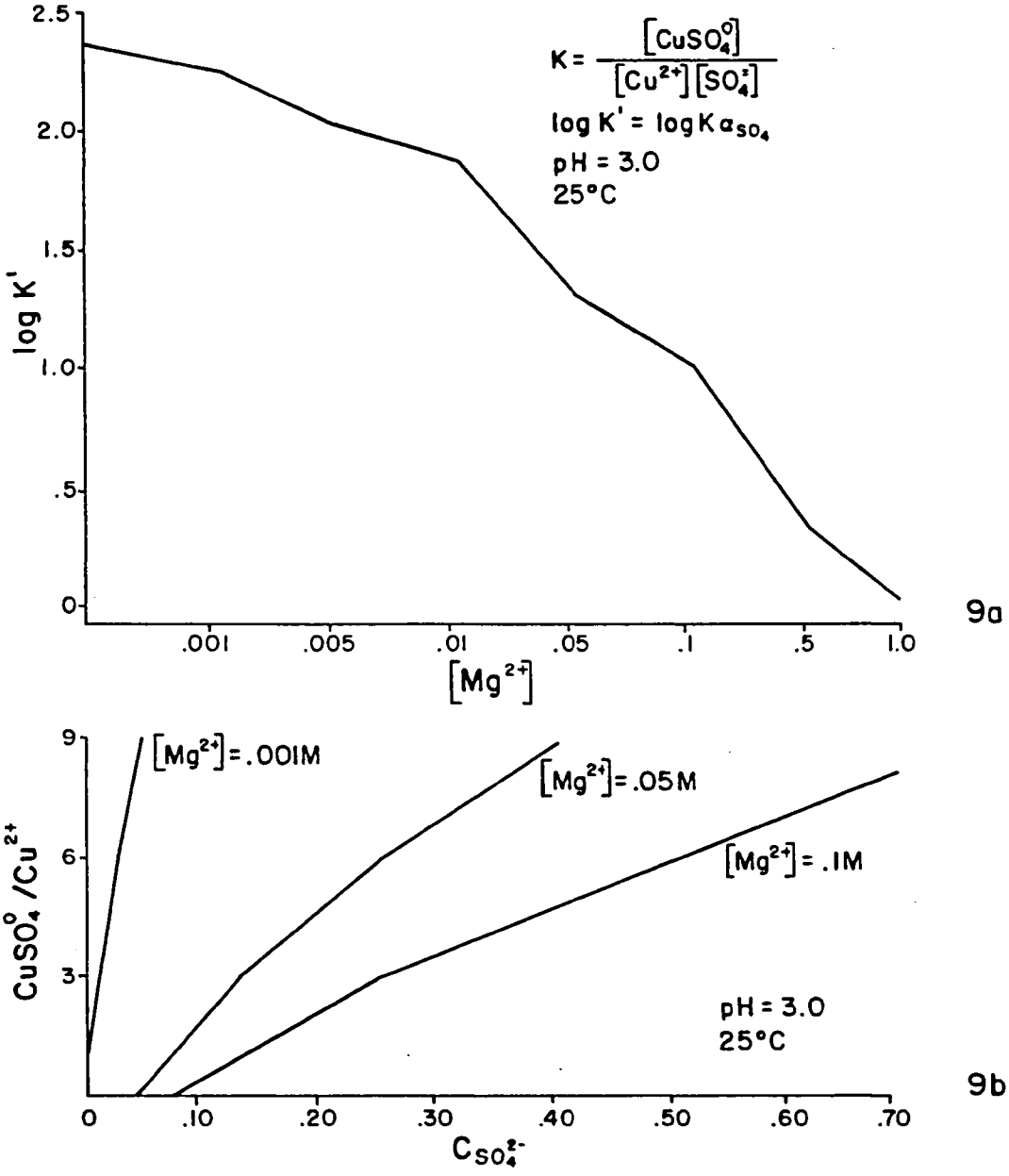

Figure 9. a) Effective change of copper sulfate complex conditional stability constant with changing Mg^{2+} concentration; b) plot of the ratio of copper sulfate to free copper with changing Mg^{2+} concentration and sulfate concentration.

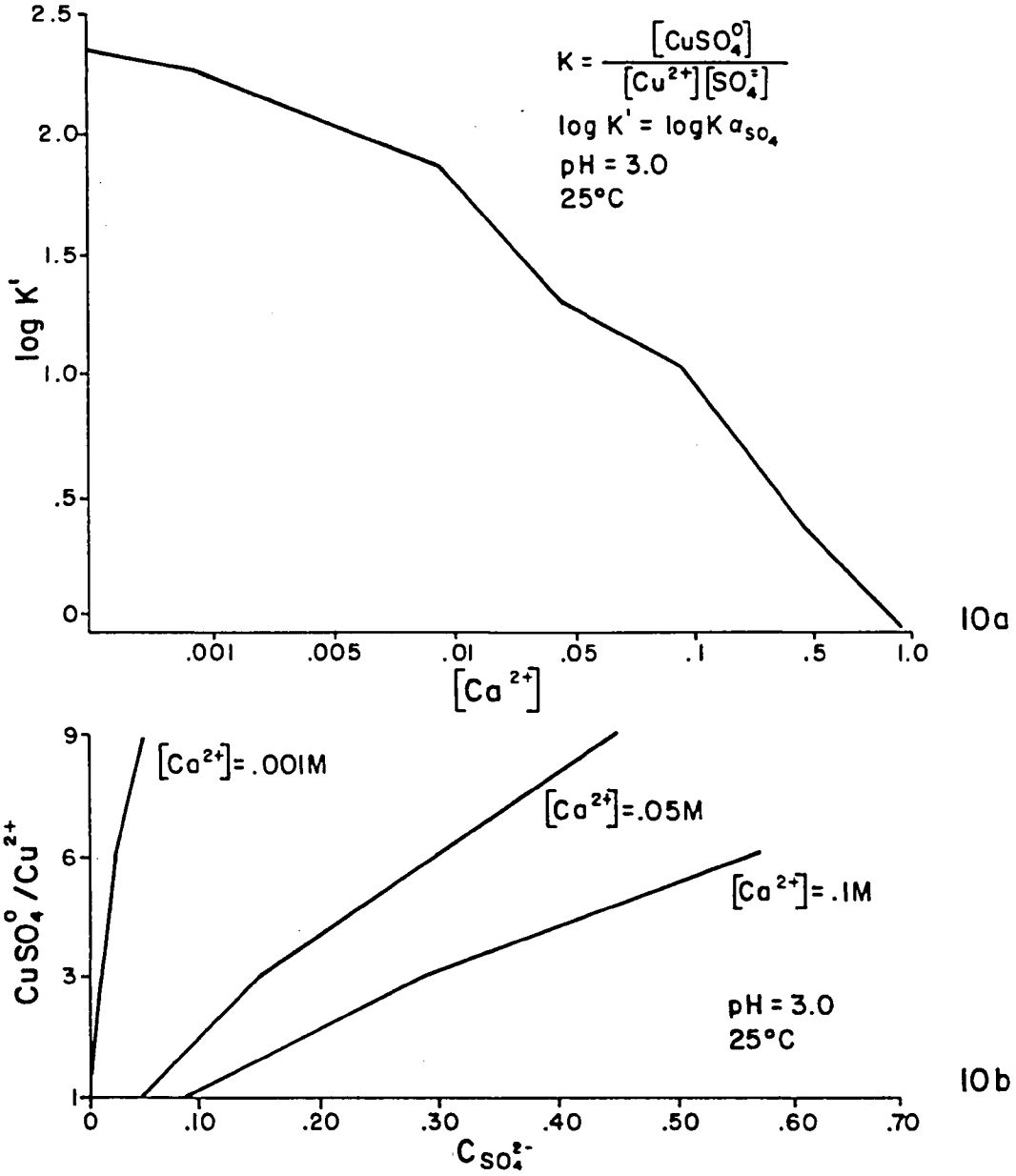

Figure 10. a) Effective change of the copper sulfate conditional stability constant with changing Ca^{2+} concentration; b) plot of the ratio of copper sulfate to free copper with changing Ca^{2+} concentration and sulfate concentration.

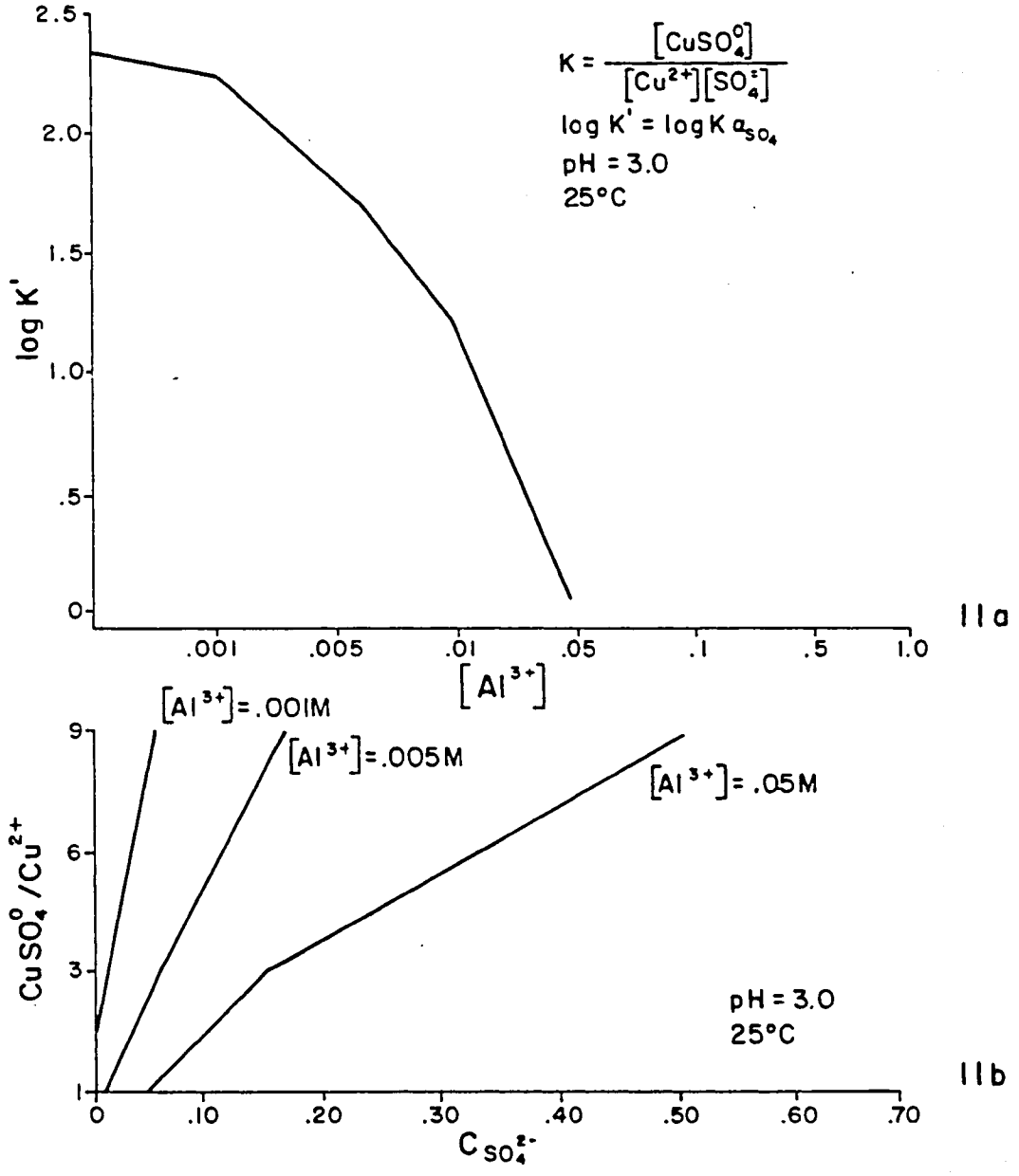

Figure 11. a) Effective change of the copper sulfate conditional stability constant with changing Al^{3+} concentration; b) plot of the ratio of copper sulfate to free copper with changing Al^{3+} concentration and sulfate concentration.

levels and subsequently will precipitate. Figure 1 graphically demonstrates that as free copper ion concentration increases, chalcanthite and cuprite will precipitate at lower and lower pH values even at high oxidation potentials. Silicate derived cations will hinder the transport of copper from the oxidized zone by driving it into equilibrium with supergene copper minerals.

These results are supported by the experiments done by Sullivan (1905). Sullivan precipitated copper from copper sulfate solutions by contact with finely ground silicate minerals. Sullivan describes the results (pg. 69);

> The between the silicate and the copper solution is chiefly an exchange of bases, copper undergoing precipitation and an equivalent quantity of other bases (chiefly the alkali and alkaline earth bases) entering the solution....The acidity of the cupric sulphate solution is not changed by contact with the silicates and precipitation copper....The sum of the bases which go into solution is exactly equivalent to the total copper precipitated,...the finer the powder the more copper is precipitated.

As verified by Sullivan's experiment the silicate derived cations form more stable complexes and therefore will replace copper in solution.

A general chemical equation that expresses the reactions of alumino-silicate clays under conditions can be written as:

$$27)\quad 3\overset{\text{solid}}{KAlMgSi_4O_{10}(OH)_2} + 8H^+ + 3(SO_4) = \overset{\text{solid}}{KAl_2AlSi_3O_{10}(OH)_2} + 3MgSO_4^0 + 9SiO_2 + 2K^+ + 6H_2O$$

This equation clearly shows how silicate reactions can decrease hydrogen and ligand activities in solution.

Because the amount of copper that can be leached from the zone of oxidation is directly proportional to hydrogen concentration and to the ligand available for copper-complexing in solution, silicate reactions have a direct effect on the efficiency of copper enrichment.

$$28)\quad \bar{n}_{\text{Cu leached}} = f(n_{H^+}(\text{pyrite oxidation}) - n_{H^+}(\text{consumed}),\ n_{\text{ligand}}(\text{pyrite oxidation}) - n_{\text{ligand}}(\text{complexed}))$$

Acid and ligand are both generated by oxidation of pyrite at high oxidation potentials. Acidity whole value is a function of total volume percent sulfide and the pyrite to chalcopyrite ratio, is modified by acid consumption in silicate site leaching and dissolution reactions. Free ligand, also produced by the oxidation of sulfides, is also modified by gangue cation complexing. The degree to which the acid and ligand is modified by the host rock depends on the host rock's reactivity which is a function of the stability of its silicate minerals in acid conditions.

CHAPTER 4

CONCLUSIONS

Silicate minerals in supergene enriched porphyry deposits alter as a result of reaction with low-temperature acid leaching solutions in patterns that correspond to copper grade levels, namely the oxidized zone, the enriched zone, and the protore zone. X-ray diffraction data shows that a 10Å mica or sericite is the dominant clay mineral in all zones of the system. Montmorillonite is present in the enriched and protore zone but has been replaced by kaolinite in the oxidized zone. The boundary between kaolinite and montmorillonite stability corresponds to the limit of the effects of high oxidation potentials, or to the limit of the oxidized zone. Chlorite is present at the interface between the enriched and protore zones and serves as a measure of the depth to which supergene attack is effective because it is stable only under neutral to alkaline conditions.

Electron microprobe analyses of the chemical compositions of individual minerals shows a definite trend in chemistry of phyllosilicate clays from the enriched zone to the oxidized zone (Figures 4-6). The relative amount of aluminum in the micas increases and silica, iron, magnesium

decreases as the effects of acid leaching become stronger. Figures 4, 5, 6a and b, indicate that leaching is removing excess cations from octahedral, tetrahedral, and interlayer sites within the mineral structure. Figure 7 plots the compositional trend of the clays from a more celadonite like composition in the enriched and protore zones to an ideal muscovite composition in the oxidized zone. Local equilibrium appears to be established in these clay size minerals by means of site leaching processes rather than through the complete dissolution of an unstable phase and the precipitation of a stable phase.

The feldspar minerals unlike the phyllosilicates show no significant change in composition with depth, however the chemical analyses may be biased because of the relatively large size of the individual crystals. The feldspars are probably altering to kaolinite along mineral surfaces especially under acidic conditions typical of the oxidized zone.

Whole rock analyses of samples shows losses of calcium, sodium, and silica and relative gains of aluminum and iron in the oxidized zone. The dominant effect of supergene reactions on the host rock is leaching of the alkali, alkali-earth, and silica cations into solution. This process is evident not only from chemical losses in the whole rock and individual minerals but also in the

gain of cations in mine water (Tables 5 and 6) relative to meteoric water.

The chemical changes that accompany the alteration of silicate minerals implies that the reactions of silicates in enriched porphyries are not separated temporally or spatially from the leaching and enrichment of copper as suggested by Bladh (1982). The mineralogic patterns of altered silicates conform too closely with supergene zonal boundaries to be coincidental notwithstanding the fact that the equilibrium kinetics of silicate clays under acidic conditions are found to be geologically fast (Clemency and Lin 1981). The lack of predicted alunite mineralization observed in leached capping could be attributed to the site leaching alteration style of clay silicates which releases less aluminum to solution than is predicted by complete dissolution of the mineral, and to the precipitation of aluminum in authigenic kaolinite. Therefore, the amount of alunite precipitated would not be directly proportional to the extent of aluminosilicate alteration in the oxidized zone as suggested by Bladh (1982), but would rather mark a degree of minimum silicate alteration.

Chemically the weathering of silicates effects the oxidation, transport, and deposition of copper sulfides in two ways, as an acid consumer and as a gangue cation contributor. During the alteration of gangue minerals acid is consumed and thereby the pH of the solution is increased.

This prevents copper migration from the oxidized zone because at higher pH values (Figure 1) copper oxide minerals are stable; thus rather than being transported to the reducing zone, copper is precipitated in the oxidized zone. An increasing activity of gangue cations will compete with copper for sulfate ligand in solution and because alkali earth-sulfate aqueous complexes are more stable than copper-sulfate complexes, sulfate ligand will preferentially complex with gangue cations leaving copper in solution as free copper ion (Figures 9-11). At high free copper concentrations (Figure 1) copper minerals will precipitate even at low pH values within the oxidized zone. The combined effect of silicate alteration in the supergene zone have a detrimental effect on the efficiency of copper leaching. Obviously, optimum levels of copper leaching will occur in rocks with a minimum of reactive silicates.

This study has several implications for in situ solution mining, where sulfuric acid is poured onto piles of low grade copper bearing rock from which solutions are collected and any copper metal is extracted. The surface area of the crushed rock on the piles is many times greater than that of the original rock which allows for very rapid silicate reaction and consequently the release of high concentrations of gangue cations when exposed to acidic solutions. Metallurgists not unexpectedly find that solution pH must be kept at extremely low values to avoid

copper oxide mineral precipitation that in turn prevents copper from concentrating in solution and blocks flow channels in the system. If a ligand such as Cl^- were added that preferentially complexes copper as opposed to the gangue cations or if a ligand were added that would form more stable complexes with the silicate cations leaving the sulfate to complex with copper, the process should become more efficient.

Finally the efficiency of the natural supergene enrichment process can be best understood as a function of both the amount of sulfide available to react and of the degree to which the host rock silicates hinder leaching. Optimum leaching would occur in areas where there is an overlap of high sulfide zones in the form of pyrite, and low silicate reactivity zones, which is best demonstrated by hypogene phyllic alteration in felsic host rocks, as at Silver Bell mine.

LIST OF REFERENCES

Anderson, J.J., 1982, Characteristics of leached capping and techniques of appraisal, in Titley, S.R., ed., Advances in Geology of the Porphyry Copper Deposits: Southwestern North America: Tucson, Arizona, The University of Arizona Press, p. 275-296.

Bence, A.E. and Albee, A.L., 1968, Empirical correction factors for the electron microanalyses of silicates and oxides: Geology, v. 76, p. 382-403.

Bladh, W.K., 1982, The formation of goethite, jarosite, and alunite during the weathering of sulfide-bearing felsic rocks: Economic Geology, v. 77, p. 176-184.

Blanchard, R., 1968, Interpretation of leached outcrops: Nevada Bureau of Mines Bulletin 66, 196 p.

Carroll, D., 1970, Clay minerals: a guide to their x-ray identification: Geological Society of America Special Paper 126, 80 p.

Clemency, C.V. and Lin, F., 1981, Dissolution kinetics of phlogopite. II Open system using and ion-exchange resin: Clays and Clay Minerals, v. 29, no. 2, p. 107-112.

Emmons, W.H., 1917, The enrichment of ore deposits: U.S. Geological Survey Bulletin 625, 530 p.

Freiser, H. and Fernando, Q., (1979), Ionic Equilibra in Analytical Chemistry: Huntington, New York, Robert E. Krieger Publishing Co., 341 p.

Garrels, R.M., 1954, Mineral species as functions of pH and oxidation-reduction potentials with special reference to the zone of oxidation and secondary enrichment of sulfide ore deposits: Geochim. Gosmochim. Acta, v. 5, p. 153-168.

Garrels, R.M. and Christ, C.L., (1965), Solutions, Minerals, and Equilibra: San Francisco, Freeman, Cooper, and Company. 450 p.

Graybeal, F., 1982, Geology of the El Tiro Area, in Titley, S.R., ed., Advances in Geology of the Porphyry Copper Deposits: Southwestern North America: Tucson, Arizona, The University of Arizona Press, p. 487-506.

Hodge, E.T., 1915, The composition of water in mines of sulphide ores: Economic Geology, v. 10, p. 123-139.

Hower, J. and Mowatt, T.C., 1966, The mineralogy of illites and mixed-layer illite/montmorillonite: American Mineralogist, v. 51, p. 825-854.

Millot, G., (1970), Geology of Clays: New York, Springler-Verlag, 429 p.

Posnak, E. and Merwin, H.E., 1922, The System Fe_2O_3- SO_3-H_2O: Journal of American Chemical Society, v. 44, p. 1965-1994.

Ransome, F.L., 1919, The copper deposits at Ray and Miami, Arizona: U.S. Geological Survey Professional Paper 115, 192 p.

Richard, K. and Courtright, J.H., 1966, Structure and mineralization at Silver Bell, Arizona, in Titley, S.R. and Hicks, C.L., eds., Geology of the Porphyry Copper Deposits: Southwestern North America: Tucson, Arizona, The University of Arizona Press, p. 157-163.

Sheppard, S.M.F., Nielson, R.L., and Taylor, H.P., Jr., 1969, Hydrogen and oxygen ratios of clay minerals from porphyry copper deposits: Economic Geology, v. 64, p. 755-777.

Siivola, J., 1969, On the evaporation of some alkali metals during the electron microprobe analyses: Bulletin of the Geological Society of Finland, v. 41, p. 85-91.

Sillen, L.G. and Martell, A.E., 1964, Stability Constants of Metal-Ion Complexes: Special Publication No. 17, The Chemical Society, London.

Stumm, W. and Morgan, J.J., 1970, Aquatic Chemistry: New York, Wiley Interscience, 583 p.

Sullivan, E.C., 1905, The chemistry of ore deposition-precipitation of copper by natural silicates: Economic Geology, v. 1, p. 67-73.

Titley, S.R., 1982, Style and progress of mineralization and alteration in porphyry copper deposits, in Titley, S.R., ed., Advances in Geology of the Porphyry Copper Deposits: Southwestern North America: Tucson, Arizona, The University of Arizona Press, p. 93-116.

Weaver, C.E. and Pollard, L.D., 1973, The chemistry of clay minerals: Developments in Sedimentology v. 15: Amsterdam, Elsevier Scientific Publishing Co.